Journal of Quaternary Science

A combined biogeochemical and paleobotanical approach to study permafrost environments and past dynamics

Journal:	*Journal of Quaternary Science*
Manuscript ID:	JQS-14-0026.R1
Wiley - Manuscript type:	Research Article
Date Submitted by the Author:	n/a
Complete List of Authors:	Ronkainen, Tiina; University of Helsinki, Environmental Sciences Väliranta, Minna; University of Helsinki, Environmental Sciences McClymont, Erin; Durham University, Geography Biasi, Christina; University of Eastern Finland, Environmental Sciences Salonen, Sakari; University of Helsinki, Geosciences and Geography Fontana, Sonia; University of Göttingen, Palynology and Climate Dynamics Tuittila, Eeva-Stiina; University of Eastern Finland, School of Forest Sciences
Keywords:	biomarker, n-alkane, macrofossil, permafrost, fen

A combined biogeochemical and paleobotanical approach to study permafrost environments and past dynamics

Corresponding author, e-mail address: tiina.m.ronkainen@helsinki.fi

Abstract

When investigating past peatland processes and related carbon cycle dynamics, it is essential to identify and separate different peat environments: bogs, fens and permafrost, and their historical plant assemblages. Bog peat layers contain relatively well-preserved plant material for palaeoecological examination, whereas fen and permafrost peats are often highly humified, which in turn constrains the reconstructions of the past plant assemblages. Here, we analyzed the chemical composition of arctic peat plateau plants to create a local reference training-set of plant biomarkers. After that we combined palaeobotanical, biogeochemical and chronological analyses to one permafrost peat sequence collected from the East European Russian tundra (67°03´N, 62°57´E) to investigate past peatland dynamics and to evaluate the performance of the biomarker method in a highly decomposed permafrost environment. Our results showed that the chronologically constrained macrofossil analysis provided most of the essential information about the peatland succession. However, a more robust reconstruction of the past peatland dynamics was achieved by combining palaeobotanical and biogeochemical data sets. The similarity of the lipid biomarker distributions of the arctic and boreal peatland plants also implies that any established modern biomarker training-set of peatland plants could be applied universally to palaeoecological studies on peat sediments.

Keywords: biomarker, *n*-alkane, macrofossil, permafrost, fen, peat plateau

1. Introduction

Peat deposits are proxy archives for the past climate and peatland dynamics, e.g., peatland expansion and carbon accumulation (Yu *et al.* 2010). When investigating past peatland processes and related carbon cycle dynamics, it is essential to identify and separate the different peat environments (bogs, fens and permafrosts), as they differ considerably in their ecohydrology i.e., the quantity, quality and physical state of water (Wheeler and Proctor, 2000; Økland *et al*., 2001). Consequently they maintain substantially different plant assemblages; dry hummock *Sphagnum* mosses and dwarf shrubs dominate bogs and the top parts of modern permafrost peat plateaus, whereas more water-demanding lawn and hollow *Sphagnum* mosses and sedges dominate fens and permafrost peat plateau depressions (e.g. Oksanen *et al*., 2001; Rydin and Jeglum 2006; Virtanen and Ek 2013). Remnants of these different peatland assemblages in historical peat deposits make it possible to separate different peatland environments when reconstructing peatland dynamics back in time (Yu *et al*., 2013). Plant macrofossils, which are partly decomposed plant material, are key to identifying past peat-forming vegetation (e.g. Barber *et al*., 1998; Mauquoy *et al*., 2002 a, b; Tuittila *et al*., 2007; Väliranta *et al*., 2007), whereas pollen analysis, which calculates inputs of different pollen grains in peat sequence, can be applied as a complementary proxy to depict wider regional-scale changes in climate and associated vegetation shifts (e.g. Kaakinen and Eronen 2000).

Typically, bog peat layers which have not been affected by permafrost contain relatively well-preserved plant material for palaeoecological examination (Väliranta *et al*., 2007), whereas fen peat and peat found in deep permafrost layers is often highly humified (Lamarre *et al.* 2012; Oksanen *et al.* 2001), which in turn constrains the identification of plant remains (e.g. Moore *et al.,* 2007; Strakova *et al*. 2011) and historical habitat reconstructions. Thus,

there is a need to identify new methods that can be applied to study these problematic highly humified layers more accurately, preferably in combination with traditional palaeobotanical proxies. Recent studies of biomarkers in boreal peat environments, conducted both by solvent extraction of total lipids and the analysis of the non-extractable residues, have shown that plant group-specific chemical compounds can be applied to identify vegetation contributions to bog peat (e.g. Abbott *et al.* 2013; Avsejs *et al*., 2002; Bingham *et al*., 2010; Jia *et al*., 2008; McClymont *et al*., 2008; Ronkainen *et al.* 2014; Xie *et al*., 2000). The most widely analyzed compounds have been the *n*-alkanes: for instance, the difference between concentrations of mid chain length (n-C_{23} and n-C_{25}) and long chain length (n-C_{29} to n-C_{33}) *n*-alkanes have been used to separate contributions of *Sphagnum* and vascular plant species in the peat (e.g. Andersson *et al*., 2011; López-Días *et al*., 2010; Ortiz *et al*., 2011; Ronkainen *et al*., 2013). However, studies focused on biomarker performance in highly humified fen peats are still scarce and accordingly it is difficult to assess the applicability of the biomarker method on highly humified peat (Andersson and Meyers 2012; Andersson *et al*., 2011; Ronkainen *et al.* 2014). The existing palaeoecological fen studies have applied information on the chemical compounds derived from modern boreal or temperate bog plants (Routh *et al*., 2014; Andersson and Meyers 2012; Andersson *et al*., 2011). Only recently has information of the biomarker composition of fen plants been introduced (Huang *et al*., 2011; Ronkainen *et al*., 2013), and so far information on arctic plants is still lacking. Here, we search for supplementary proxies to investigate highly humified peat that is typical to permafrost environments (e.g. Andersson *et al*., 2011; Oksanen *et al*., 2001; Väliranta *et al*., 2003).

Permafrost peatlands are important for the global carbon cycle, as they are estimated to store *ca.* 40% of the global soil C pool (Tarnocai *et al*., 2009). Recently their role within the global nitrogen cycle is increasingly discussed, since high N_2O emissions associated with permafrost melting (Elberling *et al*., 2010) and frost-action (Marushchak *et al*., 2011; Repo *et al*., 2009)

were discovered. Frost action, which causes cracking of the soil surface, often creates and maintains a unique surface pattern characterized by un-vegetated bare peat circles on permafrost peatlands (Bockheim and Tarnocai 1998; Seppälä 2003). Unlike the surrounding vegetated surfaces, these un-vegetated peat circles have received attention as sources of relatively high emissions of the greenhouse gas N_2O as stated above (Repo *et al*. 2009), which is the third largest greenhouse gas contributor to positive radiative forcing after CO_2 and CH_4 (IPPC 2013). The hemispheric distribution of these bare peat circles is not homogenous, but where they do occur they can be regionally quite abundant with up to 50% coverage of the land surface (Repo *et al*. 2009) (Fig. 1). The formation of the un-vegetated surfaces has vaguely been linked to cryoturbation (Repo *et al.* 2009) but real understanding of the mechanisms requires further examination of their development history. To address this issue the best possible proxy combination is needed.

In the present study, as a part of a larger project examining past, present and future C and N dynamics of permafrost peatlands characterized by un-vegetated peat circles, we aim to combine palaeobotanical (macrofossils and pollen), biogeochemical and chronological analyses to one permafrost peat core to evaluate the suitability of the biomarker method to the permafrost environments. We first assess the biomarker composition of the common peatland plants in the arctic to create a local reference training data set of plant biomarkers. The new training set will be evaluated against previous work to test whether northern peatlands have a "universal" plant biomarker distribution.

2. Material and methods

2.1. Study site and sampling

The studied peat plateau is located in the discontinuous permafrost zone in the arctic East European Russian tundra (67°03´N, 62°57´E, Komi Republic) (Fig 1), at a study site called Seida, which is located near Vorkuta city. The peat plateau is elevated a few meters from the surrounding mineral soil, and the highest parts are characterized by dwarf shrubs such as *Betula nana*, *Rhododendron tomentosum* (syn. *Ledum palustre*), *Rubus chamaemorus*, and hummock mosses *Sphagnum fuscum*, *Polytrichum strictum* and *Dicranum elongatum*. Sedges, such as *Carex aguatilis* and *Eriophorum* sp., and lawn mosses such as *Sphagnum lindbergii* dominate lower and wetter surfaces. We collected a 1.6-m-long peat sequence from a bare peat surface in summer 2012. The permafrost-free active peat layer (40 cm) was sampled with a Russian peat corer and the underlying permafrost peat with a motorized corer. The core was cut into 2-cm sample slices. Palaeobotanical, biogeochemical and chronological analyses were conducted with varying resolution from the same samples throughout the sequence. To study the biomarker composition of the most common peatland plants, we collected and analyzed the total neutral lipid fractions of 13 most representative tundra peat plateau plants collected from the vicinity of the coring point (Supplementary information Table 1).

2.2. Plant macrofossil analyses

Samples with a volume of 5 cm^3 were rinsed under running water using a 140-µm sieve, without any chemical treatment. Remains retained on a sieve were identified and proportions of different plant remains were visually estimated using a stereomicroscope (magnification of 10x) (e.g. Speranza *et al*., 2000; Mauquoy *et al*., 2002a; 2002b). More specific species identification was done using a high power light-microscope (cf. Väliranta *et al.* 2007). In

addition to identifiable plant remains, the proportion of unidentified organic matter (UOM) was estimated.

2.3. Pollen analysis

Pollen samples were prepared using standard methods described by Bennett and Willis (2001). A minimum of 1000 pollen grains and spores of terrestrial vascular plants were counted from each sample, using a light microscope with 400× magnification. After the sum of 1000 was reached, the counting was continued with only new pollen taxa recorded, together with grains of a reference taxon (*Picea abies*), to calculate percentage values for any new taxa found. Pollen taxonomy follows Bennett (2004) modified for Sweden using the checklist by Karlsson (1997).

2.4. Radiocarbon dating

Six bulk peat samples were ^{14}C dated in Poznań Radiocarbon Laboratory Poland. ^{14}C dates were calibrated in the CALIB software (Stuiver and Reimer 1993) version 7.0.0, using the IntCal13 calibration curve (Reimer *et al*. 2013). An age-depth model was calculated using the method of Heegaard *et al*. (2005) in R (version 2.15.0) (R Development Core Team 2012).

2.5. Solvent extraction

Fresh plant and peat samples for solvent extraction were freeze dried and ground to homogenous mass following the same procedure as in Ronkainen *et al*. (2013). For lipid

extraction of the samples ca. 0.2 g of sample was ultrasonicated for 20 min with 6 ml CH_2Cl_2/MeOH (3:1, v/v). Saponification of samples was conducted by adding 0.5 M methanolic (95%) NaOH and by heating the samples for 2 h at 70 °C. The neutral lipids were extracted using hexane. Activated Al_2O_3 columns were used to separate the neutral lipids into apolar and polar compounds, by eluting with hexane/CH_2Cl_2 (9:1, v/v) and CH_2Cl_2/MeOH (1:2, v/v), respectively. Prior to gas chromatography (GC) and GC-mass spectrometry (GC-MS) analysis the polar fraction of the samples were derivatised using bis(trimethylsilyl)trifluoroacetamide (Sigma Aldrich).

2.6. GC-MS

Apolar and polar fractions were analyzed using GC-MS with the gas chromatograph equipped with split/splitless injection (280 ºC). Separation was achieved with a fused silica column (30 m x 0.25 mm i.d) coated with 0.25µm 5% phenyl methyl siloxane (HP-5MS), with He as carrier gas, and the following oven temperature program: 60 – 200 °C at 20 °C/min, then to 320 °C (held 35 min) at 6°C/min. The mass spectrometer was operated in full scan mode (50-650 amu/s, electron voltage 70 eV, source temperature 230 °C). Compounds were assigned using the NIST mass spectral database and comparison with published spectra (e.g. Goad and Akihisa, 1997; Killops and Frewin, 1994). Quantification was achieved through comparison of integrated peak areas in the FID chromatograms and those of internal standards of known concentration (5-α-cholestane for apolars, 2-nonadecanone for polars). Biomarker concentrations were normalized to total organic carbon (TOC) content and are presented here as concentration per g TOC, so that samples with different extent of degradation become comparable (Meyers 2003; Ortiz *et al*., 2010).

Total organic C and N were measured by LECO TruSpec Micro CHNS-analyzer (Leco Corporation, Michigan USA) from *c.* 2 mg dried and ground samples. In a three phase analysis cycle the sample is first combusted in furnace with 1075 ºC and with He as a carrier gas flushed to the secondary oven (850 ºC) for reduction and further particulate removal. In the analyses phase the combustion gases pass the infrared detectors for CHS-measurements and Lecosorb/Anhydrone -tubes for CO_2 and H_2O removal. After that C and N are measured by thermal conductivity detector and results are computed as concentrations from the detector signal.

2.7. Statistical analyses

We applied principal component analysis (PCA) to study the variation of biomarkers within the studied fresh plant samples. In the first PCA we included all the identified compound groups: sterols, *n*-alcohols (C_{20}-C_{30}), triterpenoids and *n*-alkanes (C_{20}-C_{35}) (µg/g TOC) and *n*-alkane ratios. After that we used PCA to study the variation in the compound groups separately to compare how well they were able to separate the plant species. Prior to all the ordination analyses the biomarker data was log transformed and centered and standardized.

To relate the macrofossil and biomarker composition in the peat sequence we first clustered depth groups that share similar abundance peaks of macrofossils in the studied peat sequence using Two Way INdicator SPecies ANalysis (Twinspan for Windows 2.3). Prior to the analysis the abundances of macrofossils were standardised from 0 to 1 by setting the highest abundance of each unit to 1 and calculating other values as a percentage of the highest abundance of the unit. In the analysis we used five cut levels (0.0, 0.2, 0.4, 0.6 and 0.8) of macrofossil abundances and two division levels, which determines the maximum level of

recursive splitting for samples (Hill and Šmilauer 2005). Also, a PCA was conducted to inspect if the variation in peat biomarker data (sterols, *n*-alcohols (C_{20}-C_{28}), triterpenoids and *n*-alkanes (C_{20}-C_{35}) (µg/g TOC), and *n*-alkane ratios) relates to variation in plant macrofossil data. We applied depth groups defined by TWINSPAN as nominal supplementary variables to determinate whether the peat biomarkers show specific compounds for the depth groups constituted by the macrofossil. Similar PCA was also conducted to *n*-alkane ratios to find 10 best explaining ratios in the peat sequence. Multivariate analyses were conducted by using Canoco for Windows 4.52 (ter Braak and Smilauer 2002).

3. Results

3.1. Biomarker composition of the living tundra plants

The apolar fractions of the tundra plants were dominated by homologous series of *n*-alkanes, with minor contributions from other lipids e.g. squalene. Mixed samples of different lichen species which presently dominate peat plateaus were characterized by the domination of the C_{31} *n*-alkane together with *n*-C_{29} (Supplementary information Table 1). A moss species *Dicranum elongatum* was also dominated by *n*-C_{31}, while *Sphagnum* mosses were dominated by mid chain length alkanes *n*-C_{25} (in *S. fuscum*) and *n*-C_{23} (in *S. balticum* and *S. lindbergii*). The *n*-alkane concentrations in shrub leaves, except in *V. uliginossum*, were substantially higher (> 500 µg gTOC) than in mosses, lichens and shrub roots. In *L. palustre* and *E. nigrum* leaves *n*-C_{31} was the dominating *n*-alkane, and in *B. nana* and *V. uliginossum* leaves *n*-C_{27} dominated. Roots of *B. nana, L. palustris, E. nigrum* were dominated by *n*-C_{29} and for *V. uliginossum* roots by *n*-C_{28}. Both the leaves and roots of *R. chameamorus* were dominated by *n*-C_{27} with clearly lower concentration compared to other leaves. Long chain *n*-alkanes dominated in all studied sedges: *n*-C_{27} in *C. aquatilis* leaves and roots, *n*-C_{29} in *Eriophorum*

sp. leaves and *n*-C_{27} in *Eriophorum* sp. roots. *Betula pubescens* ssp. *czerepanovii*, syn. *Tortuosa* leaves, bark and wood matter were dominated by long-chain *n*-C_{27}. *B. pubescens* leaves clearly had the highest concentration of *n*-alkanes (*n*-C_{27} ca. 2500 µg TOCg) when compared to all studied plants (Supplementary information Table 1). Several *n*-alkane ratios have previously been proposed as means of distinguishing different inputs to peatlands. We tested these ratios for our new analyses of tundra plants, and confirm that some of the *n*-alkane ratios are able to separate *Sphagnum* mosses from the rest of the plants. Particularly effective were the ratios *n*-C_{23}/*n*-C_{27}, *n*-C_{25}/*n*-C_{29}, and *n*-C_{23}/ (*n*-C_{23}/*n*-C_{29}) . *B. nana* and *pubescens* leaves could be separated from the rest of the plants by high values of the ratio *n*-C_{23}/*n*-C_{21}. High values of the *n*-C_{25}/*n*-C_{21} ratio separated *V. uliginossum* and both *Betula* species leaves from rest of the samples . Squalene was found from all studied vascular plant samples but not in mosses or lichens. Squalene was most abundant in *R. chamaemorus* leaves, and the roots of evergreen plants roots (*E. nigrum, V. uliginossum, L. palustre*). Triterpenoids, such as taraxer-14-ene or taraxast-20-ene, were not detected in the samples (Supplementary information Table 1).

The polar fraction of the sampled plants gave mixed results. The dominating *n*-alcohol and its concentration varied in samples without any clear pattern between mosses, vascular plant roots or leaves. Phytol [(3,7,11,15-tetramethylhexadec-2-en-1-ol] was found in all other samples excluding the roots. The concentrations were highest in *R. chamaemorus* leaves and in *S. lindbergii*. Brassicasterol [(22*E*)-ergosta-5,22-dien-3β-ol] was found with greatest concentration in lichen sp., and it was only additionally detected in *D. elongatum, S. fuscum, S. balticum* and leaves of *E. nigrum.* Campesterol [campest-5-en-3β-ol] and stigmasterol [(24*E*)-stigmasta-5,22-dien-3β-ol] were found in a wider range of samples, but the concentrations were highest in *Sphagnum* mosses, *D. elongatum* and lichen spp. All samples contained β-sitosterol [(3β)-stigmast-5-en-3-ol], and the highest concentrations were found

from *B. pubescens* wood matter, *R. chamaemorus* leaves and *L. palustre* roots (Supplementary information Table 1). The polar fraction of *E. nigrum, V. uliginossum* and *B. nana* root samples were omitted from the analyses as the samples were contaminated and reliable results were not received.

3.2. Multivariate analyses of the biomarker distribution in the living tundra plants

PCA with all identified biomarkers separated the three groups: mosses, vascular plant roots and leaves along the first two axes explaining 52% of the variation (1st 30% and 2nd 22%). The concentration of most of the biomarkers showed an increasing trend towards the vascular plant leaves, with only high C_{20} *n*-alkane concentrations and a high ratio of *n*-C_{21}/*n*-C_{23} together with high campesterol and stigmasterol concentrations being typical for *Sphagnum* mosses. Lichens, *D. elongatum*, *B. pubescens* wood matter and bark grouped together with vascular plant roots (Fig 2).

Biomarker compound groups analyzed separately differed in their ability to separate plants. In the PCA with *n*-alkane concentrations, the first axis already explained 51% of the variation (Supplementary information Figure 1) and separated *E. nigrum, L. palustre* and *B. pubescens* from the rest of the sampled plants. *E. nigrum* and *L. palustre* showed high concentrations of *n*-alkanes *n*-C_{29}, *n*-C_{30}, *n*-C_{31}, *n*-C_{32} and *n*-C_{33}, and *B. pubescens* leaves have high concentration of *n*-alkanes *n*-C_{23}, *n*-C_{24}, *n*-C_{25} and *n*-C_{26}. In the PCA with *n*-alkanes ratios, the first axis explained 58% of the variation and separated clearly the *Sphagnum* mosses, and *B. nana* and *pubescens* to their own groups (Supplementary information Figure 1). In the PCA with the *n*-alcohols the first axis explained 54% of the variation. Analysis clearly separated the leaves of *B. nana* by *n*-C_{21}-ol and *n*-C_{23}-ol and *R.*

chamaemorus by *n*-C_{29}-ol from the rest of the sampled plants. Leaves of *B. pubescens*, *L. palustre, V. uliginossum* and *C. aquatilis* were separated from mosses, lichens and roots along the first axis, as the concentration of *n*-alcohols increased towards the leaves (Fig 4 d). The PCA with plant sterols and triterpenoids grouped vascular plant leaves, roots and mosses as separate clusters and the first axis explained 56% of the variation within the samples. High concentrations of squalene and β-sitosterol described the leaves, low concentrations of phytol described the roots and brassicasterol, campesterol and stigmasterol described *S. fuscum, S. balticum, D. elongatum* and lichens (Supplementary information Figure 1).

3.3. Peat sequence chronology and deposition dynamics

The radiocarbon dates reveal that the studied peat sequence does not cover the whole Holocene, and the top peat layer yielded an age 5900 cal a BP. The loss of the top part of the sequence is likely due to erosion due to permafrost initiation and associated ground uplift. Thus the studied peat sequence covers a time span 8400-5900 cal a BP (Table 1 and Fig 3). The stratification of the peat sequence shows that directly after the peat initiation, ca. 8400 cal a BP, peat deposition was very fast, nearly 1 m during the first ca. 1000 years (i.e. 1 mm a^{-1}). After 7400 cal a BP, the deposition rate slows down, to ca. 0.4 mm a^{-1}(Fig 3), which is still relatively fast rate compared to rates reported in previous studies; ca. 0.2 mm a^{-1} (e.g. Oksanen *et al*. 2001; Botch *et al*. 1995).

3.4. Plant macrofossil composition of the peat sequence

Due to the lack of the top layer the palaeobotanical composition of the whole peat core differed from the current vegetation. The palaeobotanical composition of the deepest peat sequence that contained minerotrophic bryophytes and other fen species typical of nutrient-rich conditions, such as *Filipendula ulmaria* and *Menyanthes trifoliata,* clearly indicated that until ca. 6200 cal a BP the study site was a permafrost free minerotrophic site (Fig 3). Moreover, abundant tree birch and spruce remains alongside a high number of seeds of *Carex* and *Filipendula* suggest that at first, between ca. 8300 and 7500 cal a BP, the site was a swamp or forested nutrient rich fen (zone I). After 7500 cal a BP the site became dominated by sedges and *Menyanthes* and the habitat changed to oligotrophic open fen (zone II). Vegetation composition changed abruptly ca. 6100 cal a BP. Between 6100 and 5900 cal a BP (the core top) very few identifiable plant remains were detected, although at the very surface some species that indicate dry bog conditions, such as *Empetrum nigrum* and *Dicranum* sp. were found (zone III). The amount of UOM was relatively high throughout the sequence suggesting a high level of decomposition. As an exception between ca. 7400 and 7200 cal a BP the peat was less decomposed and the amount of UOM was smaller accompanied by a high amount of sedge remains.

3.5. Pollen stratigraphy

Betula sp., *Picea* and *Cyperaceae* appeared to be the dominant pollen taxa throughout the sequence, typically together constituting 80–90% of all pollen (Fig 4). In addition, *Equisetum* and *Filipendula* reach very high values of 50–60% in single samples. These peaks likely represent highly localized, massive spore/pollen input, and coincide with abundant occurrences of *Equisetum* vegetative remains and *F. ulmaria* seeds in the macrofossil record.

3.6. Peat biomarkers

Most of the peat samples were dominated by *n*-alkanes *n*-C_{27} or *n*-C_{29} suggesting domination of vascular plant inputs (Supplementary Information Table 2). Exceptions to this dominance occurred at depths 12 cm (dominance of *n*-C_{23}), 36 cm (equally dominant *n*-C_{23}, *n*-C_{25} and *n*-C_{29}), 56cm (*n*-C_{25} and *n*-C_{21}), 64cm (*n*-C_{21}, *n*-C_{23} and *n*-C_{25}), and 72 cm (*n*-C_{23} and *n*-C_{27}). At depths 56, 64 and 72 cm the overall concentrations of *n*-alkanes were also much lower than in the rest of the analyzed core depths (Supplementary information Table 2). Variations in the *n*-alkane ratios are also identified through the peat sequence. There was little variation in the ratios between 166 and 80 cm, then between 70 to 50 cm most of the ratios increased in value, before fluctuating and decreasing towards the core top (through 50 – 0 cm, Supplementary information Figure 2). Taraxer-14-ene was found only from the very top layers of the peat core, and similarly urs-20-ene was not found from the bottom layers but only above 104 cm. In contrast, taraxast-20-ene was detected throughout the peat sequence and showed two prominent peaks at 112 and 44 cm (Supplementary information Table 2).

In the polar fraction of the peat sequence two samples, 4 and 88 cm, and the values of *n*-C_{22}-ol from all of the samples were omitted due to contamination. The *n*-alcohols formed three zones according to the dominating compounds: between 166 and 52 cm C_{28}-ol dominated most of the layers, between 144 and 128 cm *n*-C_{26}-ol dominated, at 64 cm *n*-C_{23}-ol dominated, between 48 – 32 cm there was varied domination by *n*-C_{24}-ol, *n*-C_{26}-ol and *n*-C_{28}-ol, and between 24 and 0 cm *n*-C_{24}-ol mainly dominated . β-sitosterol and the related 3-stigmastanol [(24-ethyl-5α-cholestan-3β-ol)] were present throughout the sequence, the highest concentration of β-sitosterol was detected from the sample 52 cm (14 000 µg TOCg), but overall there was no clear trend through the sequence. Campesterol and the related

campestanol [24-methyl-5α-cholestan-3β-ol] were found from sample depths 72 – 0 cm, and the campesterol concentration was highest at 0 cm (1400 µg TOCg). Stigmasterol and the related 22E-stigmastanol [(24-ethyl-5α-cholest-22-3β-ol)] were found only from the very top layers of the sequence (Supplementary information Table 2).

3.7. Plant macrofossil and biomarker distribution in the peat sequence

Based on the identified macrofossils TWINSPAN divided the studied peat sequence into three depth groups (Table 2). The first group (bog, zone III) included only the top peat sample with bog plant macrofossils. The second (swamp, zone I) and third (open fen, zone II) groups divided the fen peat sequence to peat layers with high presence of woody and other drier habitat plant macrofossils, and layers dominated by sedge and *M. trifoliata* remains as indicators of wetter habitat, respectively. When we applied the three depth groups, bog, swamp and fen, determined by the macrofossil TWINSPAN as supplementary environmental variables to a PCA for biomarkers, some depth group specific biomarkers could be pointed out in figure 5. The bog group (0cm) stands out from the other two but no specific compound described it. Depths and related biomarkers of swamp fen group was separated most clearly and described by n-C_{34}, n-C_{35}, ratio n-C_{31}/ n-C_{27}, taraxast-20-ene and phytol . In contrast, the depths and biomarkers of the fen group were situated with a wide range in the ordination space characterized by a high number of different compounds.

3.8. Degradation measures

In studying a peatland core and making comparisons to modern living plants, it is important to recognize that organic matter degradation may alter or mask the original signals produced in the plants. Consequently biomarkers may not fully reflect the organic matter sources and its preservation in peat (Zheng *et al*. 2007). Bulk density (g/cm^3), C/N ratio, and the proportion of C were all relatively stable throughout the peat sequence (Fig 3, Supplementary information Table 2). The ratio of 3-stigmastanol/β-sitosterol (Andersson and Myers, 2012), which indicates the microbially mediated degradation of sterols similarly to the 5α(H)-stanols/Δ^5-sterol ratio, stayed stable (0.3 – 0.5) through the sequence, except at depths 150, 52, 8 and 0 cm where the ratio was slightly lower, ca. 0.2. The carbon preference index (CPI: cf. Andersson and Meyers 2012), where high values are associated with well-preserved organic material (e.g. Andersson and Meyers 2012), showed some variation in the sequence, but the low values throughout the sequence in general suggest a high level of organic matter degradation (Supplementary information Table 2).

4. Discussion

4.1. Biomarkers of sub-arctic peat plateau plants

Previous studies on modern plant biomarker compositions from peatlands have concentrated on boreal and north temperate areas of Europe, excluding a recent study conducted in extreme-continental Asia (Tarasov *et al*., 2013), whereas so far data from arctic locations has been lacking. Our results show that the total lipid fractions of the studied subarctic peat plateau plants are similar to plants from more southern locations: lichens are dominated by *n*-C_{31} alkane (Ficken *et al*., 1998; Nott *et al*., 2000), *Sphagnum* mosses by *n*-C_{25} (*Sp. fuscum)* and *n*-C_{23} (*Sp. balticum* and *S. lindbergii*) (e.g. Ficken *et al*., 1998; Baas *et al*., 2000;

Bingham *et al*., 2010), *C. aquatilis* leaves by *n*-C_{27} (Ficken *et al*., 1998; Ficken *et al*., 2000; Ronkainen *et al*., 2013) and roots by *n*-C_{27}, *Eriophorum* sp. leaves by *n*-C_{29} (Nott *et al*., 2000) and roots by *n*-C_{27} (Ronkainen *et al*., 2013). Dwarf shrubs also showed similar compositions as the previous studies (Salasoo 1987; Ficken *et al*., 1998; Nott *et al*., 2000; Tarasov *et al*., 2013). Birch leaves, bark and wood were dominated by *n*-C_{27} corresponding to results reported by Sachse *et al*. (2006) and Tarasov *et al*. (2013). When the biomarker distributions of studied plants were analyzed with PCA, the *n*-alkanes, their ratios, and the sterols and triterpenoids explained the differences best, whereas *n*-alcohols were not effective as we previously observed in boreal fen plants in Finland (Ronkainen *et al*., 2013). The long chain length *n*-alkanes *n*-C_{29} to *n*-C_{33} were characteristic for evergreen shrub leaves and the mid chain length *n*-alkanes *n*-C_{23} to *n*-C_{26} described *B. pubescens* leaves rather than *Sphagnum* mosses. The reason for this pattern is the much higher total concentration of *n*-alkanes in *B. pubescens* leaves when compared to *Sphagnum* mosses. The *n*-alkane ratios such as *n*-C_{25}/*n*-C_{29}, *n*-C_{23}/*n*-C_{27}, *n*-C_{23}/ (*n*-C_{27} + *n*-C_{31}) and P_{wax} separated *Sphagnum* mosses from vascular plants, while the ratio *n*-C_{23}/ *n*-C_{21} had distinguishably high values for both *B. pubescens* and *nana* leaves. The presence of campesterol, brassicasterol and stigmasterol were indicative for mosses and lichens, while high amount of β-sitosterol and squalene was typical for vascular plant leaves, as suggested by Ronkainen *et al*. (2013) for boreal fen species. Our results imply that if the plant biomarker data is generally valid any established modern biomarker training-set of peatland plants could be universally applied to palaeoecological studies on peat archives.

4.2. Permafrost peat stratigraphy - proxy comparison

The radiocarbon and macrofossil data indicate consistent chronology and a succession from a swamp (nutrient rich forested fen) (zone I: 166-82 cm) towards a wetter and nutrient poorer open fen environment dominated by sedges (zone II: 72-8 cm) and ultimately to dry ombrotrophic bog (zone III: 4-0 cm). Statistical inspection of the macrofossil data confirmed the zonal division of the sequence (Table 2 and Fig 3). During 8400 - 6000 cal a BP the site remained permafrost free (Fig 3). The pollen data provides supportive evidence of unchanged vegetation and environmental conditions (Fig 4): although the macroscopic tree remains were not found in the record during that time period, the pollen assemblages did not change. This pollen record suggests that spruce and birch were present and there was no regional-scale environmental change as could be interpreted based only on the macrofossil record. Due to loss of the uppermost peat layer we lack the part of the deposition history that contains permafrost initiation.

The PCA with peat biomarkers and depth groups derived from macrofossil distribution was able to point out some peatland phase-related markers for the swamp phase (zone I): *n*-C_{34}, *n*-C_{35}, taraxast-20-ene, and for the open fen phase (zone II): a wide range of *n*-alkanes and *n*-alcohols, β-sitosterol and stanols. Bog (zone III) was separated as its own group but no specific biomarkers described it (Table 2, Fig 5). Interestingly, when compared to the *n*-alkane ratio compositions of the living plants, the PCA for peat (Supplementary information Figure 1) suggests the presence of *Sphagnum* mosses in the fen phase (e.g. *n*-C_{25}/*n*-C_{29}, *n*-C_{25}/ (*n*-C_{25} + *n*-C_{29}), in zone II) an important plant group forming biomass in oligotrophic fens (Laine *et al*., 2012), while the macrofossil record showed predominance of sedges and *Equisetum* (Fig 3). The *n*-alkane ratios of the peat sequence (Fig 6) also indicate a possible presence of *Sphagnum* mosses in the fen phase. This suggests that biomarkers do have potential to show occurrence of plants not seen in the traditional methods but also that several biomarker groups should be concurrently involved. A failure to detect *Sphagnum* occurrence

would act as a serious flaw for reconstruction of past C and N dynamics. The overall trend in the PCA was an increase of the number and concentration of the detected biomarkers towards the surface peat layers, which could indicate higher decomposition rate in the deeper peat layers resulting in lower lipid concentrations overall. In open fen layers (zone II), the higher P_{aq} ([n-C_{23}+n-C_{25}) / (n-C_{23}+n-C_{25}+n-C_{29}+n-C_{31}]; Ficken *et al*. 2000) values (0.6-0.7) are consistent with development of a wet fen phase in the sequence, an association also observed by Andersson *et al*. (2011) who reported similar values for wet fen phase in permafrost peat sequence. The alkane ratio n-C_{23} /(n-C_{27} + n-C_{31}) was also proposed by Andersson *et al*. (2011) to differentiate fen and bog habitats in subarctic peats, whereby ratios >0.2 would indicate bog peat and ratios <0.2 would indicate fen peat. In our study, the n-C_{23} / (n-C_{27} + n-C_{31}) ratio was not among those 23 biomarker signals that had a strong explanatory value (Fig 5). In our sequence this interpretation would suggest that swamp fen (III) and bog (I) zones both consist of bog peat, and that only the fen zone (II) is actually fen peat. Accordingly, this ratio succeeds to separate the wet open fen phase (zone II) but fails to identify the drier swamp phase (zone I) and it would rather work as an indicative marker for moisture changes than a peat type indicator, as sedges are the main component of swamp and open fen peat.

The macrofossil record suggests a change from open fen to bog environment at the top of the sequence. Although modern aeration and freeze-thaw activity is influencing the top layers, the low 3-stigmastanol/β-sitostanol ratio and high CPI value at the top peat indicates less humified peat than in the deeper layers. However, it is possible that the sparse bog plant macrofossils in the very top layers represent modern plants that have invaded the site, i.e. they do not represent the plant assemblage of 5900 cal yr BP. This interpretation is supported by the biomarker record that showed no indications of a transition from fen to bog habitat in the top layers, such as changes in n-alkane domination from long to mid chain length, n-alkane, sterols or triterpenoids concentrations, or in the n-alkane ratios (cf. Ronkainen *et al.*

2014). The shift to C_{27} *n*-alkane domination could be explained by the remains of deciduous leaves on the top layers, deposited to the surface from surrounding vegetation dominated by *B. nana* and *V. uliginossum*. Finally, the identified macrofossils on top of the peat sequence resemble the present overall dominating vegetation at the surrounding vegetated peat plateau.

In addition to the three vegetation zones both macrofossil and biomarker data showed a momentary change around 7500 – 7200 cal a BP (72 – 52 cm), which is also detected in the statistical data observation procedure which separated these depths due to association with squalene, into a sub-group within the open fen zone (Fig 5). The change is characterized by a simultaneous decrease in the amount of UOM and an increase in the amount of sedge and shrub root remains. Unlike Andersson *et al*. (2011) we did not detect a corresponding peak of C_{31} *n*-alkane with abundant shrub rootlet remains; on the contrary, the total *n*-alkane concentration decreases and the dominance of the long chain length *n*-alkanes is replaced by a switch to mid chain length *n*-alkanes (Supplementary information Table 2). This pattern suggests that either *Sphagnum* mosses, *B. pubescens* leaves or sedge roots were present (Sachse *et al*. 2006; Ronkainen *et al*. 2013), while in the macrofossil record a small amount of sedge roots (light root matter) were present (Fig 3). Furthermore, most of the studied *n*-alkane ratios and concentrations of squalene, campesterol and β-sitosterol increased, indicating an increase in vascular plant input (Ronkainen *et al.* 2014), whereas the degradation measures, 3-stigmastanol/β-sitostanol ratio and CPI value, stayed stable throughout the whole sequence (Supplementary information Table 2). The reduced *n*-alkane concentration therefore appears to be a sign of slower peat accumulation, rather than more effective degradation, as the 3-stigmastanol/β-sitostanol ratio and CPI value did not show changes in degradation (Andersson and Meyers 2012; Ronkainen *et al.* 2014). The decreased amount of UOM together with relatively high amount of sedge remains supports the proposal of lower rate of accumulation rather than fast degradation, as sedge material is suggested in

general to be degraded fast due the litter quality and related microbial and enzyme activity that is found in vascular plant litters (Bartsch and Moore 1985; Szumigalski and Bayley 1996; Strakova *et al*., 2011).

The studied permafrost peat sequence was comprised mainly from highly humified fen peat with no clear change to bog peat because it lacked the permafrost initiation event and associated shift to true bog environment. A recent study by Routh *et al*. (2014) conducted at same site on a vegetated peat plateau surface dated the permafrost initiation as late as ca. 2 200 cal a BP. Consequently, it can be hypothesized that either la great amount of organic matter has been eroded by wind from surface of the study site or that the recent peat accumulation has been extremely slow, or even some combination of these two assumed mechanisms. To resolve this further studies are required including several well-dated peat sequences from the same peatland. Despite the lost material the highly humified nature of the peat and the large amount of UOM, the macrofossil data with support from the pollen record succeeded to separate three different habitats from the studied sequence: swamp (zone I), open oligotrophic fen (zone II) and bog (zone III). The biomarker record corresponded to other proxy records: *n*-alkanes, *n*-alkane ratios, sterols and triterpenoids showed variation along the sequence. The biomarker record indicated several shifts in moisture conditions (e.g. P_{aq} and $n\text{-}C_{23}$ /($n\text{-}C_{27}$ + $n\text{-}C_{31}$)) along the sequence, and suggested that the higher plants were dominating most of the time through the presence of long chain *n*-alkanes, and the high concentrations of sterols and triterpenoids (Ronkainen *et al.* 2014). Some of the *n*-alkane ratios (e.g. $n\text{-}C_{25}/n\text{-}C_{29}$ and $n\text{-}C_{23}/n\text{-}C_{27}$) in the fen phase might also indicate the presence of *Sphagnum* mosses while the macrofossil evidence does not detect this (Supplementary information Figure 2). Thus, even though similarities in the biomarker and macrofossil data sets existed, overall the data indicate that in highly humified permafrost peat environments the macrofossils continue to be the most competitive proxy to reconstruct changes in

vegetation and local environmental conditions. An important implication of our study is that it shows the value of combining both macrofossil and biogeochemical data sets to understand better the peatland evolution - as previously suggested in several other studies (e.g. Andersson 2012; Ficken *et al*., 1998; Pancost *et al*., 2002; Ronkainen *et al.* 2014).

5. Conclusions

Our results indicate, similarly to a recent study from extreme-continental Asia (Tarasov *et al*., 2013), that lipid biomarker distributions of the common peatland plants are not affected by geographical location of the study site. If generally valid, consequently any established modern biomarker training-set of peatland plants could be universally applied to palaeoecological studies.

By applying combined biogeochemical, palaeobotanical and chronological methods we discovered a consistent permafrost peatland development history. A combination of the proxies indicated no clear transition in peat type from fen to bog peat and no signs of cryoturbation were detected. The macrofossil analyses together with the chronology largely provided the essential information about the development history of the site, while biomarkers provided information about the top core peat resembling fen rather than bog peat environment in contrast to the palaeobotanical proxy record. In addition the biomarkers indicated, unlike macrofossils, a presence of *Sphagnum* mosses in the open fen stage. Thus, a more robust reconstruction of the past peatland dynamics was best achieved by combining palaeobotanical and biochemical data.

Acknowledgements

D. Kaverin and his students are acknowledged for their help in the sample coring. We thank J. Menegazzo and M. West for the help in the laboratory, and J. Saren for conducting the element analysis. T. Virtanen is acknowledged for producing the maps in Figure 1. Funding from the Academy of Finland (codes 131409, 140863, 218101 and 201321) is acknowledged.

References:

Abbott GD, Swain EY, Muhammad AB, Allton K, Belyea LR, Laing CG, Cowie GL. 2013. Effect of water-table fluctuations on the degradation of sphagnum phenols in surficial peats. *Geochimica Et Cosmochimica Acta* **106**: 177-191.

Andersson R. 2012. Lipid biomarkers and other geochemical indicators in paleoenvironmental studies of two Arctic systems, a Russian permafrost peatland and marine sediments from Lomonosov Ridge. Doctoral thesis in Geochemistry, Stockholm University, Sweden.

Andersson RA, Meyers PA. 2012. Effect of climate change on delivery and degradation of lipid biomarkers in a Holocene peat sequence in the eastern European Russian arctic. *Organic Geochemistry* **53**: 63-72.

Andersson RA, Kuhry P, Meyers P, Zebühr Y, Crill P, Mörth M. 2011. Impacts of paleohydrological changes on n-alkane biomarker compositions of a holocene peat sequence in the eastern european russian arctic. *Organic Geochemistry* **42**: 1065-1075.

Avsejs LA, Nott CJ, Xie S, Maddy D, Chambers FM, Evershed RP. 2002. 5-*n*-Alkylresorcinols as biomarkers of sedges in an ombrotrophic peat section. *Organic Geochemistry* **33**: 861-867.

Baas M, Pancost R, Van Geel B and Sinninghe Damsté JS. 2000. A comparative study of lipids in Sphagnum species. *Organic Geochemistry* **31**: 535-541.

Barber K, Dumayne-Peaty L, Hughes P, Mauquoy D, Scaife R. 1998. Replicability and variability of the recent macrofossil and proxy-climate record from raised bogs: Field stratigraphy and macrofossil data from Bolton fell moss and Walton moss, Cumbria, England. *Journal of Quarternary Science* **13**: 515-528.

Bartsch I, Moore TR. 1985. A preliminary investigation of primary production and decomposition in four peatlands near schefferville, quebec. *Canadian Journal of Botany* **63**: 1241-1248.

Bennett K, Willis K. 2001. Pollen. In: Tracking environmental change using lake sediments. Terrestrial, algal, and siliceous indicators. Vol.3. Terrestrial, algal, and siliceous indicators. Smol J.P., Birks H.J.B., Last W.M. edn. Dordrecht, TheNetherlands: Kluwer Academic Publishers

Bennett K. 2004. Pollen catalogue of the British Isles. (http://chrono.qub.ac.uk/pollen/pc-intro.html)

Bingham EM, McClymont EL, Väliranta M, Mauquoy D, Roberts Z, Chambers FM, *et al*. 2010. Conservative composition of n-alkane biomarkers in Sphagnum species: Implications for palaeoclimate reconstruction in ombrotrophic peat bogs. *Organic Geochemistry* **41**: 214-220.

Bockheim JG, Tarnocai C. 1998. Recognition of cryoturbation for classifying perma-frost-affected soils. *Geoderma* **81**: 281–293.

Botch MS, Kobak KI, Vinson TS, Kolchugina TP. 1995. Carbon pools and accumulation in peatlands of the former Soviet Union, *Global Biogeochemical Cycles* **9**: 37-46.

Elberling B, Christiansen HH, Hansen BU. 2010. High nitrous oxide production from thawing permafrost. *Nature Geoscience* **3**: 332-335.

Ficken KJ, Barber KZ, Eglinton G. 1998. Lipid biomarker, δ 13C and plant macrofossil stratigraphy of a Scottish montane peat bog over the last two millennia. *Organic Geochemistry* **28**: 217-237.

Ficken KJ, Li B, Swain DL, Eglinton G. 2000. An *n*-alkane proxy for the sedimentary input of submerged/floating freshwater aquatic macrophytes. *Organic Geochemistry* **31**: 745-749.

Goad LJ, Akihisa T. 1997. *Analysis of sterols*. Blackie Academic and Professional, Blackie Academic and Professional, London.

Heegaard E, Birks HJB, Telford RJ. 2005. Relationships between calibrated ages and depth in stratigraphical sequences: an estimation procedure by mixed-effect regression. *The Holocene* **15**:612.618.

Hill MO, Šmilauer P. 2005. WinTWINS version 2.3. Availeble at http://planet.uwc.ac.za/nisl/computing/Twinspan/userguide_twinspan.pdf (accessed 12 September 2013).

Huang X, Wang C, Zhang J, Wiesenberg GLB, Zhang Z, Xie S. 2011. Comparison of free lipid compositions between roots and leaves of plants in the Dajiuhu Peatland, Central China. *Geochemical Journal* **45**: 365-373.

IPCC, 2013: Climate Change 2013: The Physical Science Basis. Contribution of Working Group I to the Fifth Assessment Report of the Intergovernmental Panel on Climate Change [Stocker, T.F., D. Qin, G.-K. Plattner, M. Tignor, S.K. Allen, J. Boschung, A. Nauels, Y. Xia, V. Bex and P.M. Midgley (eds.)]. Cambridge University Press, Cambridge, United Kingdom and New York, NY, USA, 1535 pp.

Jia G, Dungait JAJ, Bingham EM, Väliranta M, Korhola A, Evershed RP. 2008. Neutral monosaccharides as biomarker proxies for bog-forming plants for application to palaeovegetation reconstruction in ombrotrophic peat deposits. *Organic Geochemistry* **39**: 1790-1799.

Kaakinen A, Eronen M. 2000. Holocene pollen stratigraphy indicating climatic and tree-line changes derived from a peat section at ortino, in the pechora lowland, northern russia. *Holocene* **10**: 611-620.

Karlsson T. 1997. Förteckning over svenska kärlväxter. The vascular plants of Sweden- a checklist. *Svensk Botanisk Tidskrift* **91**: 241-560.

Killops SD, Frewin NL. 1994. Triterpenoid diagenesis and cuticular preservation. *Organic Geochemistry* **21**: 1193-1209.

Laine A, Bubier J, Riutta T, Nilsson MB, Moore TR, Vasander H, Tuittila E-S. 2012. Abundance and composition of plant biomass as potential controls for mire net ecosytem CO 2 exchange. *Botany* **90**: 63-74.

Lamarre A, Garneau M, Asnong H. 2012. Holocene paleohydrological reconstruction and carbon accumulation of a permafrost peatland using testate amoeba and macrofossil analyses, Kuujjuarapik, subarctic Quebec, Canada. *Review of palaeobotany and palynology*, **186** (SI): 131-141.

López-Días V, Borrego T, Blanco CG, Arboleya M, López-Sáez JA, López-Merino L. 2010. Biomarkers in a peat deposit in Northern Spain (Huelga de Bayas, Asturias) as proxy for climate variation. *Journal of Chromatography A* **1217**: 3538-3546.

Mauquoy D, Engelkes T, Groot MHM, Markesteijn F, Oudejans MG, Van Der Plicht J., *et al*. a 2002. High-resolution records of late-Holocene climate change and carbon accumulation in two north-west European ombrotrophic peat bogs. *Palaeogeography, Palaeoclimatology, Palaeoecology* **186**: 275-310.

Mauquoy D, Van Geel B, Blaauw M, Van der Plicht J. b 2002. Evidence from northwest European bogs shows 'Little Ice Age' climatic changes driven by variations in solar activity. *Holocene* **12**: 1-6.

Marushchak ME, Pitkämäki A, Koponen H, Biasi C, Seppälä M, Martikainen PJ. 2011. Hot spots for nitrous oxide emissions found in different types of permafrost peatlands. *Global Change Biology* **17**: 2601-2614.

McClymont EL, Mauquoy D, Yeloff D, Broekens P, Van Geel B, Charman DJ., *et al*. 2008. The disappearance of Sphagnum imbricatum from Butterburn Flow, UK. *Holocene* **18**: 991-1002.

Meyers PA. 2003. Applications of organic geochemistry to paleolimnological reconstructions: A summary of examples from the Laurentian Great Lakes. *Organic Geochemistry* **34**: 261-289.

Moore TR, Bubier JL, Bledzki L. 2007. Litter decomposition in temperate peatland ecosystems: The effect of substrate and site. *Ecosystems*,**10**: 949-963.

Nott CJ, Xie S, Avsejs LA, Maddy D, Chambers FM, Evershed RP. 2000. *n*-Alkane distributions in ombrotrophic mires as indicators of vegetation change related to climatic variation. *Organic Geochemistry* **31**: 231-235.

Oksanen PO, Kuhry P, Alekseeva RN. 2001. Holocene development of the Rogovaya River peat plateau, European Russian Arctic. *Holocene* **11**: 25-40.

Ortiz JE, Díaz-Bautista A, Aldasoro JJ, Torres T, Gallego JLR, Moreno L, *et al*. 2011. *n*-Alkan-2-ones in peat-forming plants from the Roñanzas ombrotrophic bog (Asturias, northern Spain). *Organic Geochemistry* **42**: 586-592.

Ortiz JE, Gallego JLR, Torres T, Díaz-Bautista A, Sierra C. 2010. Palaeoenvironmental reconstruction of Northern Spain during the last 8000 cal yr BP based on the biomarker content of the Roñanzas peat bog (Asturias). *Organic Geochemistry* **41**: 454-466.

Pancost RD, Baas M, Van Geel B, Sinninghe Damsté JS. 2002. Biomarkers as proxies for plant inputs to peats: An example from a sub-boreal ombrotrophic bog. *Organic Geochemistry* **33**: 675-690

R Development Core Team (2012). R: A language and environment for statistical computing. R Foundation for Statistical Computing, Vienna, Austria. http://www.R-project.org/.

Reimer PJ, Bard E, Bayliss A, Beck JW, Blackwell PG, Bronk Ramsey C, Buck CE, Cheng H, Edwards RL, Friedrich M, Grootes PM, *et al*. 2013. IntCal13 and MARINE13 radiocarbon age calibration curves 0-50000 years calBP. *Radiocarbon* **55**:1869-1887.

Repo ME, Susiluoto S, Lind SE, Jokinen S, Elsakov V, Biasi C, Virtanen T, Martikainen PJ. 2009. Large N_2O emissions from cryoturbated peat soil in tundra. *Nature Geoscience* **2**: 189-192.

Ronkainen T, McClymont EL, Väliranta M, Tuittila E-S. 2013. The *n*-alkane and sterol composition of living fen plants as a potential tool for palaeoecological studies. *Organic Geochemistry* **59**: 1-9.

Ronkainen T, McClymont EL, Tuittila E-S, Väliranta M. 2014. Plant macrofossil and biomarker evidence of fen–bog transition and associated changes in vegetation in two Finnish peatlands. *Holocene in press* **24**: 828-841.

Routh J, Hugelius G, Kuhry P, Filley T, Kaislahti-Tillman P, Becher M, Crill P. 2014. Multi-proxy study of soil organic matter dynamics in permafrost peat deposits reveal vulnerability to climate change in the European Russian Arctic. *Chemical Geology* **368**: 104-117, ISSN 0009-2541, http://dx.doi.org/10.1016/j.chemgeo.2013.12.022.

Rydin H, Jeglum JK. 2006. *The Biology of Peatlands.* Oxford: Oxford University Press.

Sachse D, Radke J, Gleixner G. 2006. dD values of individual n-alkanes from terrestrial plants along a climatic gradient - Implications for the sedimentary biomarker record. *Organic Geochemistry* **37**: 469-483.

Salasoo I. 1987. Epicuticular wax alkanes of some heath plants in central Alaska. *Biochemical Systematics and Ecology* **15**: 105–107

Seppälä M. 2003. Surface abrasion of palsas by wind action in Finnish Lapland. *Geomorphology* **52**:141–148.

Speranza A, Van Der Plicht J, Van Geel B. 2000. Improving the time control of the Subboreal/Subatlantic transition in a Czech peat sequence by 14C wiggle-matching. *Quaternary Science Reviews* **19**: 1589-1604.

Strakova P, Niemi RM, Freeman C, Peltoniemi K, Toberman H, Heiskanen I, Laiho R. 2011. Litter type affects the activity of aerobic decomposers in a boreal peatland more than site nutrient and water table regimes. *Biogeosciences* **8**: 2741-2755.

Stuiver M, Reimer PJ. 1993. Extended 14C Data Base and Revised Calib 3.0 14C Age Calibration Program. *Radiocarbon* **35**:215-230.

Szumigalski AR, Bayley SE. 1996. Decomposition along a bog to rich fen gradient in central alberta, canada. *Canadian Journal of Botany* **74**: 573-581.

Tarasov PE, Müller S, Zech M, Andreeva D, Diekmann B, Leipe C. 2013. Last glacial vegetation reconstructions in the extreme-continental eastern Asia: Potentials of pollen and n-alkane biomarker analyses. *Quaternary International* **290-291**: 253-263.

Tarnocai C, Canadell JG, Schuur EAG, Kuhry P, Mazhitova G, Zimov S. 2009. Soil organic carbon pools in the northern circumpolar permafrost region. *Global Biogeochemical Cycles* **23**: 11.

Tuittila E-S, Väliranta M, Laine A, Korhola A. 2007. Controls of mire vegetation succession in a southern boreal bog. *Journal of Vegetation Science* **18**: 891-902.

ter Braak CJFP, Šmilauer P. 2002. CANOCO reference manual and CanoDraw for Windows user's guide: Software for canonical community ordination (version 4.5). NY, Ithaca: Microcomputer Power.

Virtanen T, Ek M. 2013. The fragmented nature of tundra landscape. *International Journal of Applied Earth Observation and Geoinformation* **27**: 4-12.

Väliranta M, Kaakinen A, Kuhry P. 2003. Holocene climate and landscape evolution east of the Pechora Delta, East-European Russian Arctic. *Quaternary Research* **59**: 335-344.

Väliranta M, Korhola A, Seppä H, Tuittila E-S, Sarmaja-Korjonen K, Laine J, *et al*. 2007. High-resolution reconstruction of wetness dynamics in a southern boreal raised bog, Finland, during the late Holocene: A quantitative approach. *Holocene* **17**: 1093-1107.

Wheeler BD, Proctor MCF. 2000. Ecological gradients, subdivisions and terminology of north-west European mires. *Journal of Ecology* **88**: 187-203.

Yu Z, Loisel J, Brosseau DP, Beilman DW Hunt SJ. 2010. Global peatland dynamics since the last glacial maximum. *Geophysical Research Letters* **37**(13).

Yu Z, Loisel J, Turetsky MR, Cai S, Zhao Y, Frolking S, *et al*. 2013. Evidence for elevated emissions from high-latitude wetlands contributing to high atmospheric CH4 concentration in the early Holocene. *Global Biogeochem Cycles* **27**:131-40.

Xie S, Nott CJ, Avsejs LA, Volders F, Maddy D, Chambers FM, *et al*. 2000. Palaeoclimate records in compound-specific δD values of a lipid biomarker in ombrotrophic peat. *Organic Geochemistry* **31**: 1053-1057.

Zheng Y, Zhou W, Meyers PA, Xie S. 2007. Lipid biomarkers in the zoigê-hongyuan peat deposit: Indicators of holocene climate changes in west china. *Organic Geochemistry* **38**: 1927-1940.

Økland RH, Okland T, Rydgren K. 2001. A Scandinavian perspective on ecological gradients in north-west European mires: Reply to Wheeler and Proctor. *Journal of Ecology* **89**: 481-486.

Map of the site and the bare peat circles. Maps produced by T. Virtanen; satellite image based on QuickBird © DigitalGlobe; Distributed by Eurimage/Pöyry.
142x147mm (300 x 300 DPI)

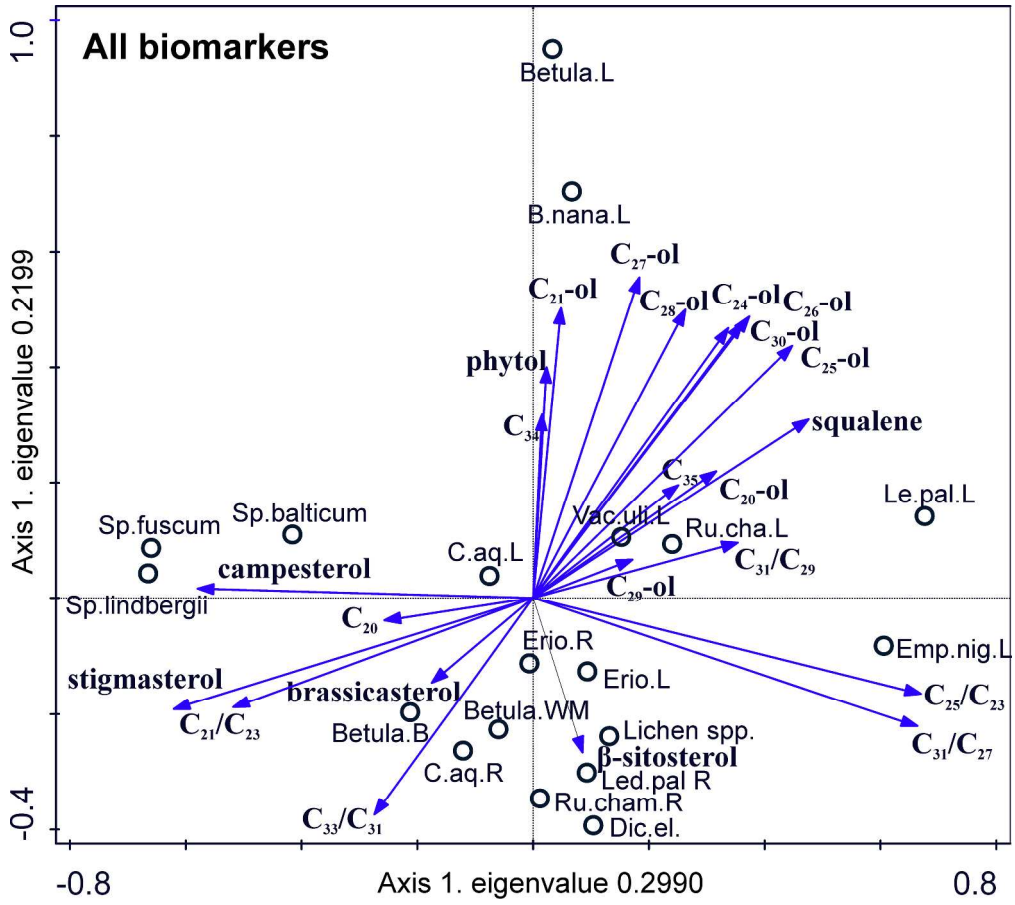

PCA of living plant biomarkers. All detected biomarkers combined first two axes explain 52% of the variation, in the figure 50% (n=23) best explaining biomarkers are shown.
165x147mm (600 x 600 DPI)

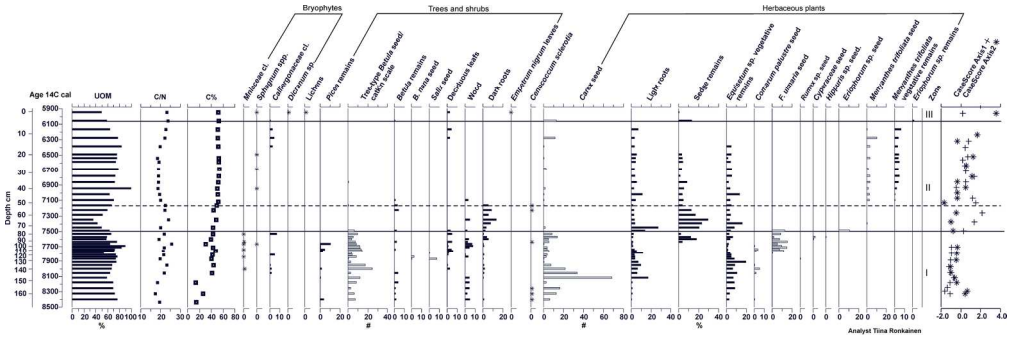

Plant macrofossils of the peat sequence. Black bars represent percentage coverages, grey bars represent counted values, macrofossils with star symbol the percentage coverage was 1 % or less. Ages are calibrated BP years. Marked zones I: swamp fen, II: fen, III: bog. Case score Axis 1 and 2 are case scores of axis 1 and 2 from peat biomarker PCA (Fig 5). Dashed line marks zone within fen zone where UOM is low and amount of sedges is high.
95x31mm (600 x 600 DPI)

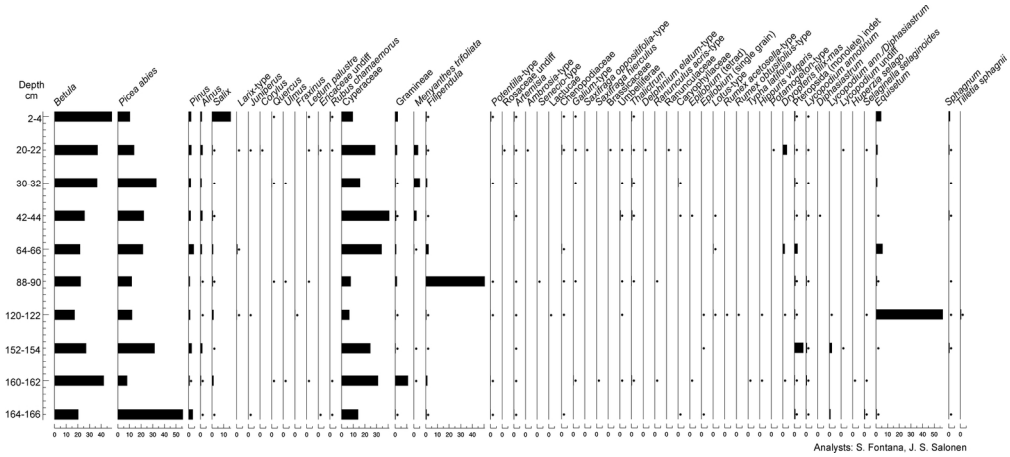

Pollen record of the sequence.
81x36mm (600 x 600 DPI)

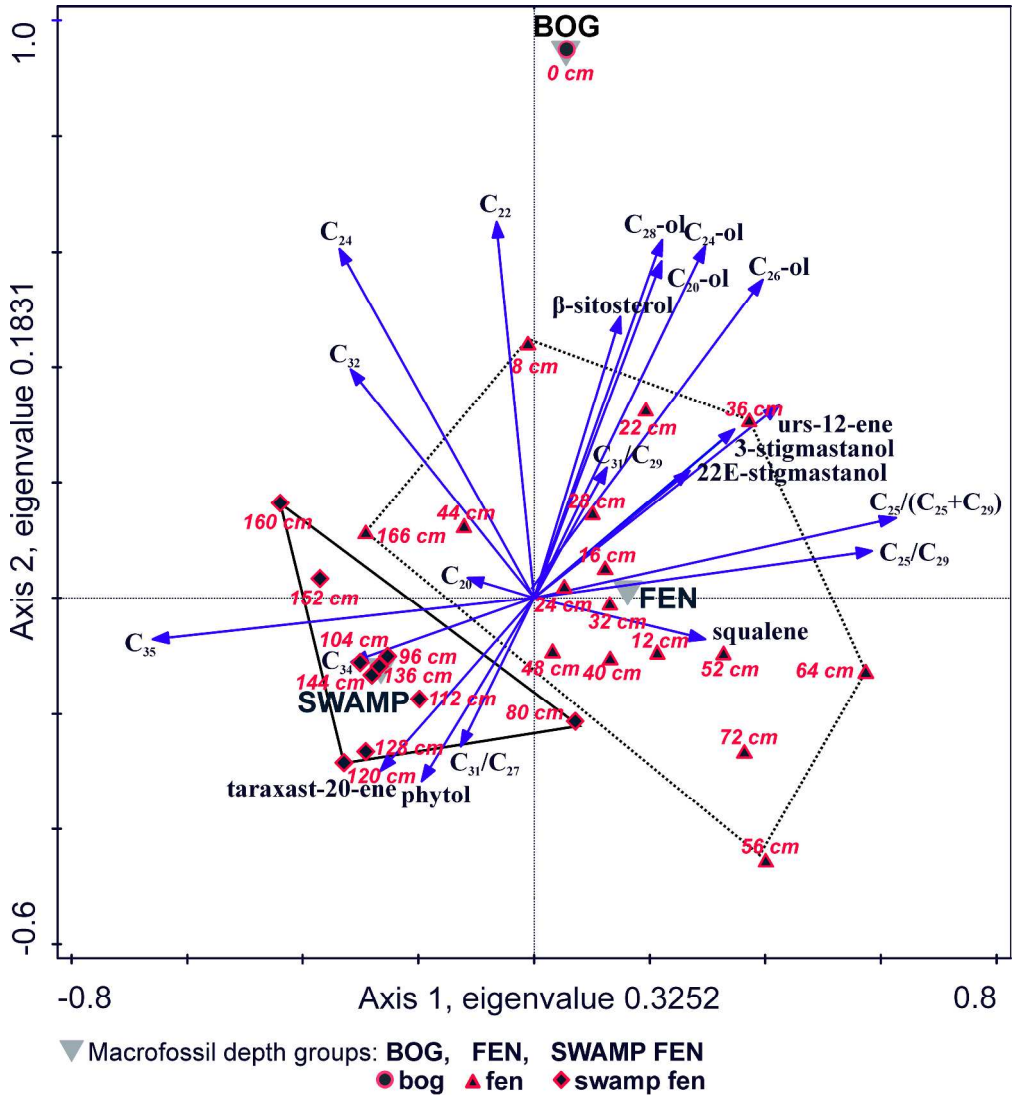

PCA ordination of the biomarkers in the peat sequence. First two axes explain 51% of the variation. Biomarkers explaining 50% (n=23) of the variation are shown. Depth groups (swamp, fen, bog) derived from macrofossil TWINSPAN analyses are used as supplementary environmental variables.
218x238mm (600 x 600 DPI)

Radiocarbon results and corresponding ages. Dated material is from bulk peat sample.

Lab code	Depth (cm)	14C age (14C yr BP ±)	Calibrated age (cal yr BP, 95% probability)
Poz-53596	0	5220 ± 1σ 35	5930 - 5992
Poz-53598	26	5840 ± 1σ 40	6570 - 6727
Poz-53599	54	6300 ± 1σ 40	7176 - 7264
Poz-53600	82	6690 ± 1σ 40	7511 - 7592
Poz-54230	110	6960 ± 1σ 50	7719 - 7844
Poz-54231	138	7140 ± 1σ 40	7940 - 7997
Poz-54232	166	7670 ± 1σ 50	8410 - 8517

LEVEL 1	LEVEL 2
	n=11 Group 00 Sample depth cm: **80, 88, 96, 104, 112, 120, 128, 136, 144, 152, 160** dark root, deciduous leaves, wood, *Picea* remains, *C. palustre* seeds, *Betula* seeds, *F. ulmaria* seeds
n=28 Sample depth cm: **4, 8, 12, 16, 22, 24, 28, 32, 36, 40, 44, 48, 52, 56, 64, 72, 80, 88, 96, 104, 112, 120, 128, 136, 144, 152, 160, 166** *Calliergonaceae,* shrub root, light root, *Betula* remains, *Equisetum* veg. remains, *M. trifoliata* veg.remains, *Carex* seeds, *M. trifoliata* seeds, Betula seeds	**n=17 Group 01** Sample depth cm: **4, 8, 12, 16, 22, 24, 28, 32, 36, 40, 44, 48, 52, 56, 64, 72, 166** sedge remains, *M. trifoliata* veg.remains, *M. trifoliata* seeds
n=1 Group 0 Sample depth cm: **0** *Sphagnum* spp., *Dicranum* spp., Lichen spp., *E. nigrum* , deciduous leaves, wood	
Division 1: n=29, eigenvalue 0.300	Division 2 (groups 00 and 01): n=28, eigenvalue 0.243

Plant samples		*n*- alkanes			
Sample	**Habitat**	**C18**	**C19**	**C20**	**C21**
Betula tree L	mineral soil	nd	nd	0.5	17.9
B.nana L	peat plateau hummock	nd	nd	0.2	6.3
Rubus chameamorus L	peat plateau hummock	nd	nd	0.7	1.5
Carex aquatilis L	fen	nd	0.8	0.6	3.8
Eriophorum sp. L	fen	nd	nd	0.4	4.8
Vaccinium uliginossum L	peat plateau hummock	nd	nd	nd	0.4
Ledum palustre L	peat plateau hummock	nd	nd	nd	0.9
Empetrum nigrum L	peat plateau hummock	nd	nd	nd	0.5
B.nana R	peat plateau hummock	nd	nd	0.2	0.3
R. chameamorus R	peat plateau hummock	nd	nd	0.1	0.3
C.aquatilis R	fen	nd	nd	0.2	0.9
Eriophorum s p. R	fen	nd	nd	0.3	2.6
V. uliginossum R	peat plateau hummock	nd	nd	nd	nd
L. palustre R	peat plateau hummock	nd	nd	0.3	0.9
E. nigrum R	peat plateau hummock	nd	nd	0.2	0.3
Betula tree WM	mineral soil	nd	0.1	0.2	0.6
Betule tree B	mineral soil	1.9	4.1	6.0	8.2
Lichen spp.	peat plateau hummock	nd	0.2	0.2	0.5
Dicranum elongatum	peat plateau hummock	nd	0.3	0.2	0.8
Sphagnum fuscum	peat plateau hummock	nd	0.3	0.2	86.9
Sp.balticum	fen	nd	2.1	0.6	38.7
Sp.lindbergii	fen	nd	0.7	0.2	20.2

Tree *Betula = Betula pubescens* ssp. *Czerepanovii,* syn. *Tortuosa*
not detected = nd
sample omitted = -
L = leaves
R = roots
WM = wood matter
B = bark

Supplementary information 1.
Plant biomarker data.

C22	C23	C24	C25	C26	C27	C28	C29	C30	C31	C32
21.0	1141.6	88.5	1510.2	96.6	2565.1	34.4	319.7	24.3	248.0	11.0
7.4	489.8	33.6	550.3	29.9	844.7	20.0	171.9	13.5	306.6	9.0
11.4	2.3	14.0	24.7	11.9	43.7	11.9	21.9	4.4	9.6	4.4
2.8	18.4	14.9	17.5	13.2	58.2	13.3	27.1	7.2	8.8	4.4
2.0	12.5	11.3	31.8	11.1	66.5	12.3	101.4	8.1	40.6	4.4
1.2	9.2	15.8	42.9	11.4	127.0	11.9	15.7	6.5	7.3	3.1
0.9	11.8	8.1	40.9	12.1	102.3	34.5	1448.0	66.1	1623.1	47.4
0.7	7.2	6.1	24.3	6.5	156.4	20.0	852.8	47.3	1552.3	40.5
0.7	2.9	4.7	5.2	4.2	6.9	6.3	7.2	4.9	5.9	2.9
1.2	4.3	8.0	8.5	7.7	10.9	7.6	10.7	6.1	8.1	2.7
1.5	6.6	10.8	11.5	11.0	13.9	9.6	10.4	6.2	5.8	3.5
2.5	14.1	14.0	24.9	16.7	45.6	18.9	40.1	13.4	20.0	9.6
1.3	4.4	8.4	8.4	8.6	10.0	11.3	10.0	7.8	8.1	4.2
1.0	4.6	7.7	10.1	10.6	12.0	10.0	17.2	6.9	15.1	4.1
0.8	2.5	5.3	5.5	5.3	8.2	7.0	68.8	3.5	46.4	2.5
1.6	6.7	7.3	12.1	7.0	15.9	13.4	9.1	4.9	4.2	3.3
5.7	9.2	11.4	14.4	9.3	24.3	8.0	10.7	8.9	7.8	5.0
1.2	4.0	7.6	10.3	11.2	15.7	12.3	24.9	9.6	31.8	4.9
1.0	4.0	8.3	9.6	8.6	10.5	5.8	34.4	5.6	59.3	3.2
4.1	103.5	11.5	133.6	11.2	59.5	5.0	11.8	2.1	9.4	1.5
3.7	66.4	14.1	44.2	18.4	33.2	28.2	27.4	24.0	21.0	13.5
2.8	45.4	8.1	21.8	8.7	11.7	7.9	7.8	4.1	4.8	2.8

			n- alkane ratios				
C33	C34	C35	C23/C25	C23/C27	C23/C29	C23/C31	C25/C29
21.3	6.6	2.6	0.8	0.4	3.6	4.6	0.6
29.7	1.2	0.8	0.9	0.6	2.8	1.6	0.7
4.5	2.2	1.7	0.1	0.1	0.1	0.2	0.6
3.1	2.7	1.6	1.0	0.3	0.7	2.1	0.3
5.3	3.5	2.0	0.4	0.2	0.1	0.3	0.5
3.3	1.8	1.4	0.2	0.1	0.6	1.3	0.3
355.0	2.4	1.9	0.3	0.1	0.0	0.0	0.4
539.9	3.7	2.2	0.3	0.0	0.0	0.0	0.2
2.1	1.3	0.9	0.6	0.4	0.4	0.5	0.7
3.3	1.5	0.9	0.5	0.4	0.4	0.5	0.8
3.1	2.0	1.1	0.6	0.5	0.6	1.1	0.8
6.0	4.9	2.1	0.6	0.3	0.4	0.7	0.5
2.9	2.1	0.9	0.5	0.4	0.4	0.5	0.8
3.3	1.3	1.6	0.5	0.4	0.3	0.3	0.8
3.5	1.2	0.7	0.5	0.3	0.0	0.1	0.7
1.7	1.9	1.1	0.6	0.4	0.7	1.6	0.8
3.4	2.9	1.4	0.6	0.4	0.9	1.2	0.6
9.2	2.8	2.0	0.4	0.3	0.2	0.1	0.7
11.6	1.5	0.8	0.4	0.4	0.1	0.1	0.9
2.3	1.6	0.5	0.8	1.7	8.8	11.0	2.2
9.5	6.9	4.7	1.5	2.0	2.4	3.2	1.3
2.2	1.9	0.9	2.1	3.9	5.8	9.4	1.9

C31/C27	C31/C29	C33/C31	C23/(C23+C29)	C25/(C25+C29)	C23/(C27+C31)
0.1	0.8	0.1	0.8	0.8	0.4
0.4	1.8	0.1	0.7	0.8	0.4
0.2	0.4	0.5	0.1	0.5	0.0
0.2	0.3	0.4	0.4	0.4	0.3
0.6	0.4	0.1	0.1	0.2	0.1
0.1	0.5	0.5	0.4	0.7	0.1
15.9	1.1	0.2	0.0	0.0	0.0
9.9	1.8	0.3	0.0	0.0	0.0
0.8	0.8	0.4	0.3	0.4	0.2
0.7	0.8	0.4	0.3	0.4	0.2
0.4	0.6	0.5	0.4	0.5	0.3
0.4	0.5	0.3	0.3	0.4	0.2
0.8	0.8	0.4	0.3	0.5	0.2
1.3	0.9	0.2	0.2	0.4	0.2
5.6	0.7	0.1	0.0	0.1	0.0
0.3	0.5	0.4	0.4	0.6	0.3
0.3	0.7	0.4	0.5	0.6	0.3
2.0	1.3	0.3	0.1	0.3	0.1
5.6	1.7	0.2	0.1	0.2	0.1
0.2	0.8	0.2	0.9	0.9	1.5
0.6	0.8	0.5	0.7	0.6	1.2
0.4	0.6	0.5	0.9	0.7	2.8

Paq	ACL C19-C35	Pwax	C23/C21	C21/C23	C25/C21	C25/C23
0.8	26.0	0.5	63.9	0.0	84.5	1.3
0.7	26.4	0.6	77.5	0.0	87.1	1.1
0.5	27.5	0.7	1.5	0.7	16.0	10.6
0.5	26.9	0.7	4.9	0.2	4.7	1.0
0.2	28.0	0.8	2.6	0.4	6.6	2.5
0.7	26.8	0.7	23.1	0.0	107.9	4.7
0.0	30.2	1.0	13.2	0.1	45.6	3.5
0.0	30.5	1.0	15.7	0.1	52.9	3.4
0.4	28.1	0.7	9.3	0.1	16.4	1.8
0.4	28.0	0.7	16.1	0.1	32.2	2.0
0.5	27.3	0.6	7.7	0.1	13.3	1.7
0.4	27.6	0.7	5.5	0.2	9.7	1.8
0.4	27.9	0.7		0.0		1.9
0.3	28.3	0.8	5.1	0.2	11.3	2.2
0.1	29.4	0.9	9.9	0.1	21.7	2.2
0.6	27.0	0.6	10.7	0.1	19.3	1.8
0.6	26.2	0.6	1.1	0.9	1.8	1.6
0.2	29.1	0.8	7.7	0.1	20.0	2.6
0.1	29.6	0.9	5.0	0.2	12.1	2.4
0.9	24.2	0.3	1.2	0.8	1.5	1.3
0.7	25.5	0.4	1.7	0.6	1.1	0.7
0.8	24.4	0.3	2.2	0.4	1.1	0.5

Sterol/triterpenoid						
squalene	taraxer-14-ene	phytol	brassicasterol	campesterol	stigmasterol	β-sitosterol
160.0	nd	nd	nd	nd	nd	70343.8
31.3	nd	nd	nd	nd	nd	6609.5
449.7	nd	nd	nd	nd	nd	2600.4
21.0	nd	nd	nd	212.7	nd	7707.1
16.3	nd	5209.0	nd	55.7	nd	nd
190.7	nd	7309.5	nd	827.5	246.2	17494.8
73.1	nd	4835.7	nd	704.8	214.6	6192.5
13.5	nd	284190.2	nd	nd	nd	139915.0
92.7	nd	nd	-	-	-	-
1.1	nd	1647.4	nd	28.0	nd	2989.5
9.1	nd	10575.3	nd	nd	nd	5210.3
18.0	nd	1460.4	68.1	nd	nd	3307.8
210.5	nd	-	-	-	-	-
211.1	nd	1215.3	68.6	3172.6	2791.0	3994.3
414.4	nd	-	-	-	-	-
327.2	nd	nd	nd	257.8	24.9	4814.4
13.9	nd	nd	nd	nd	nd	26757.1
nd	nd	828.1	2994.7	3831.5	10807.4	1546.6
nd	12.5	122409.4	nd	87996.1	70963.1	50805.9
nd	2.2	893.2	nd	nd	nd	288448.1
nd	nd	646.6	nd	nd	nd	54058.6
nd	nd	nd	nd	126.7	66.2	4348.4

	n- alcohols						
3-stigmastanol	C20-ol	C21-ol	C22-ol	C23-ol	C24-ol	C25-ol	C26-ol
1465.1	124.5	nd	nd	nd	79.9	nd	nd
290.4	nd	nd	nd	nd	nd	nd	nd
277.9	nd	nd	nd	nd	nd	nd	nd
673.1	nd	nd	nd	nd	213.6	nd	420.0
nd	242.6	18.5	1177.4	97.5	1153.0	nd	491.6
326.9	nd	nd	nd	nd	60.7	nd	108.9
131.9	nd	nd	nd	nd	86.7	nd	346.8
nd	1134.0	nd	2589.1	nd	11608.9	778.1	82238.3
-	-	-	-	-	-	-	-
80.0	26.5	nd	1792.0	73.1	768.3	61.5	346.3
nd	221.4	nd	135.8	11.9	864.1	33.6	619.2
nd	35.3	nd	101.6	nd	513.8	nd	386.8
-	-	-	-	-	-	-	-
nd	nd	nd	nd	nd	31.2	nd	nd
-	-	-	-	-	-	-	-
90.6	nd	nd	nd	nd	nd	nd	nd
nd	39.2	nd	nd	nd	nd	nd	nd
nd	nd	nd	nd	nd	nd	nd	nd
nd	nd	nd	nd	nd	3768.4	nd	4604.0
58609.5	1082.6	nd	nd	nd	nd	nd	nd
nd	nd	nd	nd	nd	nd	nd	nd
136.9	nd	nd	nd	nd	nd	nd	nd

C27-ol	C28-ol	C29-ol	C30-ol
nd	nd	nd	nd
nd	nd	nd	nd
nd	nd	nd	nd
nd	983.0	nd	1517.4
44.8	541.4	nd	66.3
nd	122.6	nd	nd
72.4	7457.9	nd	220.9
1981.1	52463.2	832.6	5781.2
-	-	-	-
56.8	326.0	nd	19.3
106.5	652.1	nd	nd
nd	191.9	nd	nd
-	-	-	-
nd	nd	nd	nd
-	-	-	-
nd	nd	nd	nd
nd	nd	nd	nd
nd	nd	nd	nd
nd	1467.6	nd	nd
nd	nd	nd	nd
nd	nd	nd	nd
nd	nd	nd	nd

Peat samples					Sterol/triterpenoid			
Depth	C%	C/N	Bulk density	CPI	squalene	taraxer-14-ene	urs-12-ene	taraxast-20-ene
0 cm	52.6	23.4	0.16	7.5	0.9	15.5	2.9	3.8
4 cm	53.0	24.0	0.15	7.1	0.3	7.9	2.8	4.0
8 cm	51.5	22.8	0.10	6.7	1.1	4.7	2.0	2.0
12 cm	51.1	22.3	0.09	5.3	2.2	nd	nd	1.6
16 cm	52.4	19.8	0.07	3.6	69.6	nd	5.4	2.0
22 cm	52.9	18.5	0.08	5.0	0.9	nd	2.2	3.3
24 cm	53.2	19.4	0.07	5.0	nd	nd	1.6	3.4
28 cm	54.0	19.0	0.10	4.9	1.1	nd	5.3	4.7
32 cm	53.0	19.2	0.09	4.6	0.5	nd	5.0	5.4
36 cm	52.2	19.0	0.12	3.3	0.6	nd	2.7	7.0
40 cm	50.6	18.9	0.09	4.8	0.3	nd	1.9	9.2
44 cm	51.6	19.7	0.14	2.2	1.0	nd	2.0	10.0
48 cm	52.3	20.1	0.07	4.4	0.5	nd	2.5	7.7
52 cm	49.7	22.5	0.00	3.8	2.1	nd	1.6	4.3
56 cm	44.1	22.2	0.08	2.4	1.9	nd	1.5	4.4
64 cm	48.5	24.1	0.07	2.3	2.3	nd	nd	6.5
72 cm	43.4	20.2	0.06	3.2	0.9	nd	0.9	5.3
80 cm	43.4	21.9	0.08	10.9	1.2	nd	2.7	4.8
88 cm	39.6	19.4	0.06	3.2	0.7	nd	2.3	8.1
96 cm	31.0	25.7	0.16	6.1	0.7	nd	nd	7.7
104 cm	43.1	22.1	0.08	6.7	1.0	nd	4.2	10.8
112 cm	47.6	21.4	0.08	6.4	1.6	nd	nd	11.3
120 cm	42.7	21.9	0.08	5.3	0.8	nd	nd	8.1
128 cm	40.7	19.9	0.08	5.9	1.1	nd	nd	4.6
136 cm	44.1	23.5	0.10	6.6	1.1	nd	nd	5.4
144 cm	42.0	22.1	0.09	3.3	0.7	nd	nd	7.5
152 cm	14.3	18.5	0.25	3.2	nd	nd	nd	4.6
160 cm	26.7	17.6	0.18	3.2	nd	nd	nd	5.3
166 cm	14.9	19.5	0.00	4.7	nd	nd	nd	3.4

not detected = nd
sample omitted = -
C22-ol concentrations are omitted from the analysis due contamination of the detected peak in GC-MS

Supplementary information 2.
Peat biomarker data.

phytol	campestrol	campestanol	stigmasterol	22E-stigmasterol-22-en-3β-ol	β-sitosterol	3-stigmastanol	3-stigmastanol/ β-sitosterol
nd	1388.7	nd	663.5	nd	10791.6	2107.7	0.2
-	-	-	-	-	-	-	
136.1	244.4	nd	71.9	nd	2735.2	699.4	0.2
34.8	106.1	56.4	nd	nd	686.4	272.1	0.3
178.9	136.1	87.5	nd	nd	808.6	522.5	0.4
915.6	301.9	229.2	nd	nd	3064.6	1481.2	0.3
156.4	113.5	99.2	nd	nd	769.5	485.9	0.4
296.1	175.2	131.6	nd	nd	1012.0	886.5	0.5
165.6	129.4	73.5	nd	nd	663.3	610.5	0.5
536.2	202.2	186.2	88.3	135.1	1187.6	986.6	0.5
140.2	85.7	59.5	nd	nd	659.4	671.6	0.5
150.9	101.7	nd	nd	nd	528.5	459.7	0.5
336.8	nd	nd	nd	nd	1043.1	911.0	0.5
159.2	434.1	nd	nd	nd	14020.1	2604.5	0.2
12.7	42.6	35.8	nd	nd	787.3	500.5	0.4
113.0	420.4	293.8	nd	nd	2782.2	2331.1	0.5
98.7	214.1	113.5	nd	nd	1006.3	1135.7	0.5
345.3	nd	nd	nd	nd	1540.7	891.9	0.4
-	-	-	-	-	-	-	
374.7	nd	nd	nd	nd	2483.6	2206.6	0.5
227.9	nd	nd	nd	nd	612.1	425.5	0.4
453.7	nd	nd	nd	nd	1202.9	952.6	0.4
169.4	nd	nd	nd	nd	521.1	393.3	0.4
148.4	135.8	nd	nd	nd	804.4	464.0	0.4
162.6	nd	nd	nd	nd	1478.6	630.3	0.3
148.7	nd	nd	nd	nd	1013.2	659.2	0.4
440.0	nd	nd	nd	nd	4281.2	961.5	0.2
142.5	nd	nd	nd	nd	1813.4	693.6	0.3
104.8	nd	nd	nd	nd	913.9	372.8	0.3

***n*- alcohols**

C20-ol	C21-ol	C22-ol	C23-ol	C24-ol	C25-ol	C26-ol	C27-ol	C28-ol
1284.0	405.4	-	707.1	5392.6	313.1	3387.5	360.1	2884.8
-	-	-	-	-	-	-	-	-
344.3	80.9	-	106.3	1046.0	46.1	679.1	62.1	478.6
37.0	5.2	-	nd	63.1	nd	49.5	nd	58.6
48.0	14.6	-	14.7	110.6	nd	126.2	nd	124.8
300.6	69.2	-	nd	1671.3	88.9	1160.8	90.5	715.9
45.0	10.4	-	nd	90.2	nd	86.1	nd	72.8
79.4	11.9	-	15.4	222.0	nd	189.2	nd	140.2
29.6	7.9	-	nd	81.6	nd	89.8	nd	97.3
168.5	32.7	-	43.0	1511.3	51.3	1355.6	53.0	978.3
27.1	15.1	-	nd	80.9	nd	143.5	nd	127.5
24.0	20.0	-	nd	55.4	nd	81.1	nd	93.3
nd	nd	-	nd	165.6	nd	248.2	nd	193.7
144.5	nd	-	nd	397.6	nd	282.4	nd	467.5
8.9	nd	-	nd	nd	nd	nd	nd	nd
103.1	190.7	-	491.9	35.7	nd	233.8	190.7	181.5
105.8	15.3	-	14.1	144.7	nd	120.2	nd	227.8
28.2	nd	-	nd	74.4	nd	69.5	nd	86.7
-	-	-	-	-	-	-	-	-
50.6	nd	-	nd	97.5	nd	nd	nd	149.1
41.5	nd	-	nd	35.4	nd	37.9	nd	45.6
44.3	nd	-	nd	47.5	nd	54.3	nd	76.8
18.1	nd	-	nd	37.3	nd	30.4	nd	39.9
30.3	nd	-	nd	31.9	nd	44.1	nd	37.9
32.1	nd	-	nd	63.9	nd	76.7	nd	128.4
33.5	nd	-	nd	60.0	nd	84.3	nd	72.5
nd	nd	-	nd	nd	nd	nd	nd	nd
76.4	nd	-	nd	95.2	nd	71.8	nd	149.5
426.5	nd	-	nd	nd	nd	nd	nd	297.0

C30-ol
274.2
-
55.2
nd
nd
120.3
nd
74.1
23.6
167.9
nd
nd
nd
nd
nd
nd
41.3
nd
-
nd
nd
nd
nd
nd
nd
nd
nd
nd
nd

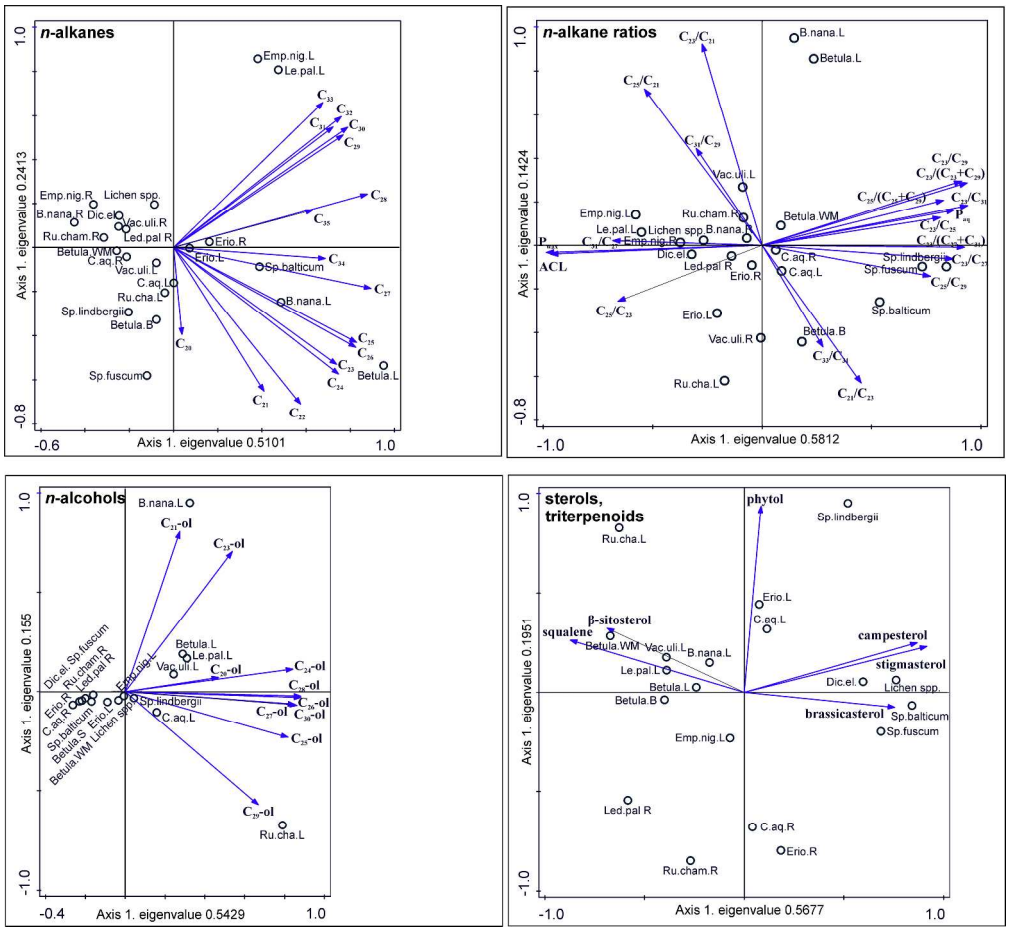

PCA of living plant biomarkers: for *n*-alkanes first two axes explain 75% of the variation; for *n*-alkane ratios first two axes explain 72% of the variation; for *n*-alcohols ratios first two axes explain 69% of the variation; for sterols and triterpenoids first two axes explain 76 % of the variation.
203x187mm (600 x 600 DPI)

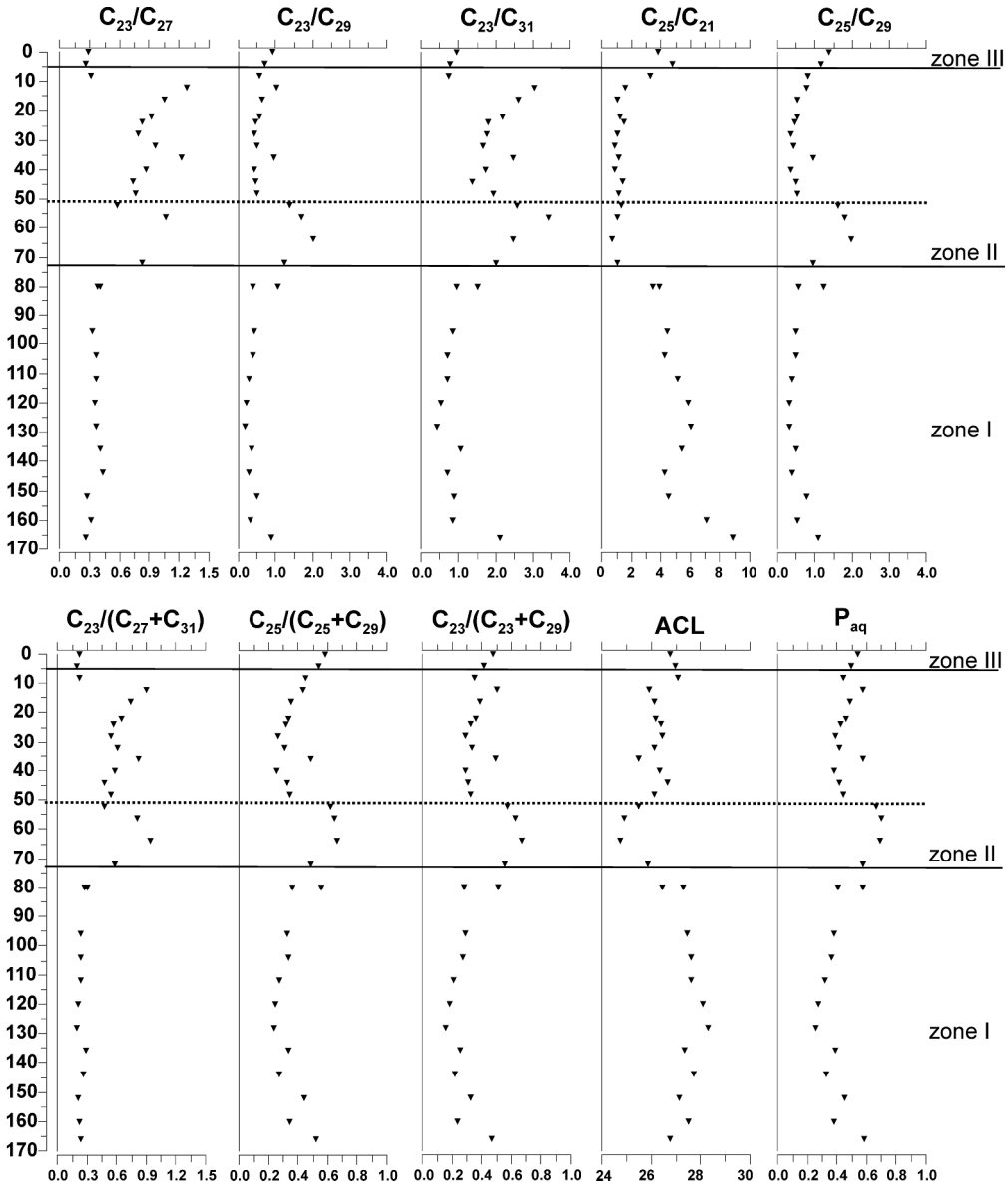

10 best fitted (PCA for peat ratios) *n*-alkane ratios of peat sequence. Marked zones according to the macrofossil data; I: swamp fen, II: fen, III: bog. Dashed line marks zone within fen zone where UOM is low and amount of sedges is high
182x214mm (600 x 600 DPI)